Pak. J. Engg. & Appl. Sci. Vol. 4, Jan 2009 (p. 1-14)

Earthquake Response Evaluation of RC Frames using High Strength Steel

A.U. Qazi[1], M. Ilyas[1], L. P. Ye[2]

[1] *Civil Engineering Department, University of Engineering and Technology Lahore, Pakistan..*
[2] *Civil Engineering Department, Tsinghua University, Beijing, China.*

Abstract

To achieve better structural performance, lesser damage along with minimum residual displacements is a main objective of earthquake resistant design. In ordinary steel reinforced concrete frames, chances of severe damage because of the lower strength of conventional steel are always present during strong earthquakes. With the invention of high-strength steel (HSS) it can be anticipated that its introduction in the structures will reduce the degree of damage against strong motions. However, its role towards improved seismic behavior needs to be investigated. In order to realize the response benefits against earthquakes three, six and ten story two bays bare concrete frames reinforced with HSS in columns are compared with the equivalent ordinary steel reinforced frames. Nonlinear static pushover and time history analysis are performed. The results reveal that the HSS reinforced frames have more lateral resistance with reduced residual displacements. Yielding at the column ends and probable story failure mechanisms are prevented. It is envisaged that efficient use of HSS in columns can yield safer structures. Further the potential danger of complete collapse can be reduced.

Key words: damage; residual displacements; earthquake; high-strength steel; frames; columns; mechanism; reinforced concrete

1. Introduction

Despite advances in recent years it is still difficult to predict the characteristics of future earthquakes. Failures in 1994 Northridge and 1995 Kobe earthquakes demonstrate the need to search new materials and systems to built safer structures. In an ordinary frame construction probable failure mechanisms may include total failure mechanism with weak beams, with weak columns, soft story and partial mechanism as shown in Figure 1[1]. Plastic hinges at the columns bases are necessary to initiate frame sway [2]. In moment resistant frame, designed according to the strong column and weak beam philosophy plastic hinges are confined to the beams ends and at the first story columns bases. Since ordinary reinforcements have limited yield strength and elastic strain limit, significant yielding of the ordinary reinforcements in columns results in the formation of failure mechanisms. Further disadvantages of ordinary reinforcements are large residual deformations in frames and excessive rehabilitation demands after strong shaking [3]. Structural systems with self centering abilities have

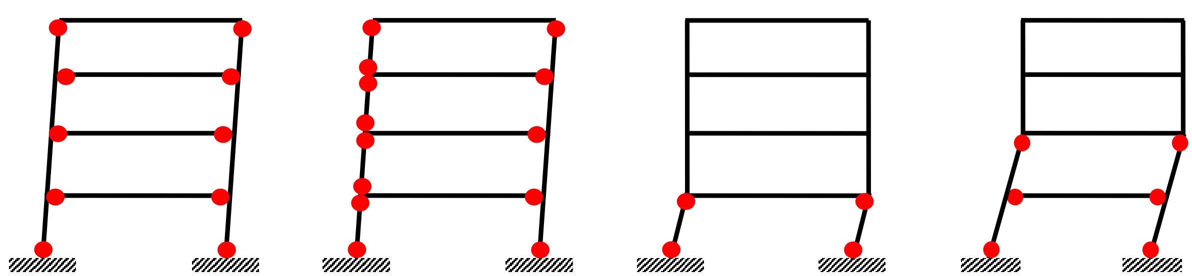

(a) Total mechanism with weak beams **(b)Total mechanism with weak columns** **(c) Soft story mechanism** **(d) Partial mechanism**

Figure 1: Failure Mechanisms of Reinforced Concrete Frames

utilized un-bonded post tensioned steel tendons in precast concrete [4, 5, 6] in steel structures [7] and in concrete bridge piers [8]. Furthermore, advanced composite materials have also been investigated [3].

Stiffness plays much lower role than strength in resisting failure mechanisms during seismic event [9]. Steel yield strength is an important factor in determining the flexural strength of reinforced concrete structural members. Therefore upon reaching of the yield strength and under cyclic loadings the flexural stiffness rapidly deteriorates. In earthquake resistant frames, deformation demands for columns may vary due to the uncertainties in the prediction of future earthquake motions. Increase in column-to-beam strength ratio although reduces possibility of story failure mechanism [10]. However, ordinary reinforcements in columns cannot provide large flexural strength and elastic deformation capacity. It is likely that under large lateral sway column section will go into inelastic range. Therefore to avoid formation of plastic hinges in columns and to eliminate the chances of soft story and partial failure mechanisms, HSS reinforcement in columns is studied here. The response benefits as a result of these numerical investigations are reported and are compared with the corresponding ordinary steel reinforced concrete frames. With the simple proposed damage markers the degree of damage in both the ordinary and HSS reinforced frames is also evaluated.

2. Frames Geometry and steel area ratios

In this study, three, six and ten story two bay bare frames are analyzed. The floor beams were loaded with a uniformly distributed load of 30kN/m. The analyzed frame geometries are shown in Fig. 2(a). The benchmark frames, named as ordinary frames (OFs), are designed according ACI 318-02 [11] by using the conventional steel. The cross section details and longitudinal reinforcement ratios are given in table 1. For comparison the ordinary reinforcements in columns are replaced with HSS and are designated as Passive Frames (PFs).

3. Finite element models, material models and analysis methods

Frames are modeled on MSC.MARC finite element code. For section behavior fiber model THUFIBER [12, 13] is used. THUFIBER fiber model is a general purpose program and has ability of solving nonlinear problems.

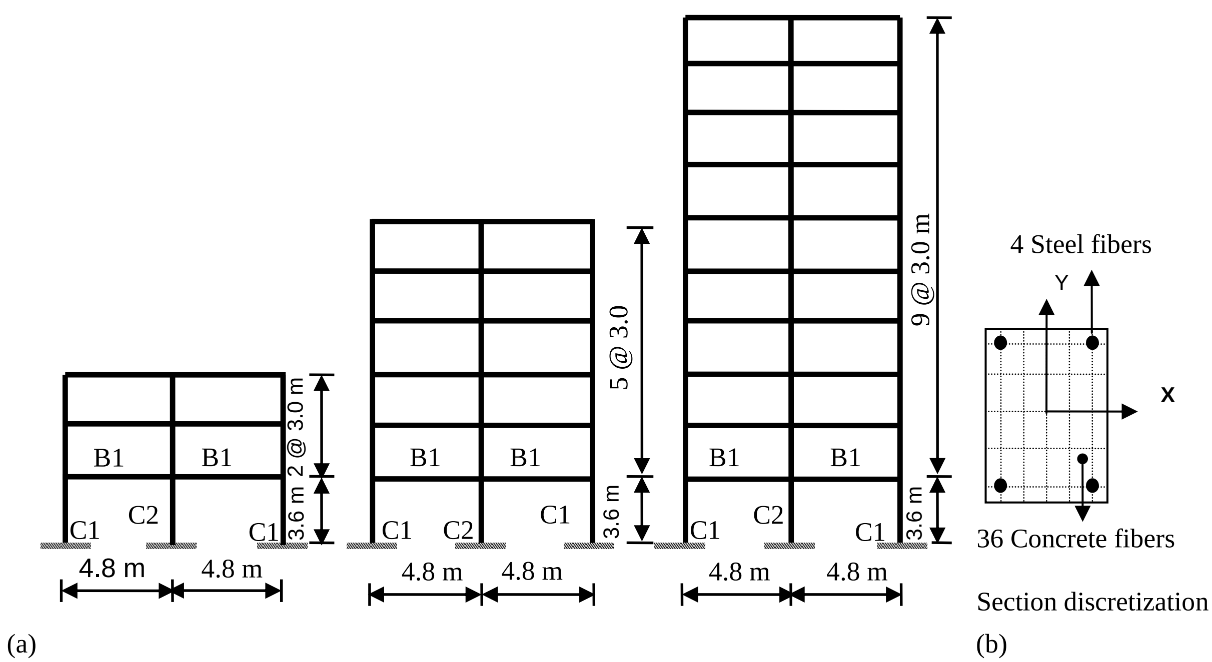

Figure 2: (a) Geometry of frames and (b) section descritization elements

Table 1: Geometric details and longitudinal reinforcement ratios (ρ, %)

Frame	Story/ Floor	Column		Beam	
		Sections (mm)	ρ^a (%)	Sections (mm)	ρ^b (%)
three story	1st	C1 (400X400)	1.0	B1 (250X450)	1.0
		C2 (400X450)	1.3		
	2nd	C1 (400X400)	1.0	B1 (250X450)	1.0
		C2 (400X450)	1.3		
	3rd	C1 (400X400)	1.0	B1 (250X450)	0.9
		C2 (400X450)	1.2		
six story	1st	C1 (400X450)	1.0	B1 (250X450)	1.1
		C2 (400X500)	1.2		
	2nd	C1 (400X450)	1.0	B1 (250X450)	1.1
		C2 (400X500)	1.2		
	3rd	C1 (400X400)	1.0	B1 (250X450)	1.0
		C2 (400X450)	1.2		
	4th	C1 (400X400)	1.0	B1 (250X450)	1.0
		C2 (400X450)	1.2		
	5th	C1 (400X400)	1.0	B1 (250X450)	1.0
		C2 (400X450)	1.2		
	6th	C1 (400X400)	1.0	B1 (250X450)	0.9
		C2 (400X450)	1.2		
ten story	1st	C1 (400X475)	1.0	B1 (300X450)	1.1
		C2 (400X550)	1.2		
	2nd	C1 (400X475)	1.0	B1 (300X450)	1.1
		C2 (400X500)	1.2		
	3rd	C1 (400X450)	1.0	B1 (250X450)	1.0
		C2 (400X500)	1.2		
	4th	C1 (400X450)	1.0	B1 (250X450)	1.0
		C2 (400X500)	1.2		
	5th	C1 (400X450)	1.0	B1 (250X450)	1.0
		C2 (400X500)	1.2		
	6th	C1 (400X450)	1.0	B1 (250X450)	0.9
		C2 (400X500)	1.2		
	7th	C1 (400X400)	1.0	B1 (250X450)	0.9
		C2 (400X450)	1.2		
	8th	C1 (400X400)	1.0	B1 (250X450)	0.9
		C2 (400X450)	1.2		
	9th	C1 (400X400)	1.0	B1 (250X450)	0.9
		C2 (400X450)	1.2		
	10th	C1 (400X400)	1.0	B1 (250X450)	0.8
		C2 (400X450)	1.2		

[a] Total area of steel/Gross section area
[b] Area of tension steel/Effective section area

Each section of the beams and columns is discretized into 36 concrete and 4 steel fibers one at each corner of the cross section, as shown in Figure 2 (b). The clear cover of concrete is 25mm assumed. For core concrete in compression a uni-axial compressive stress-strain model which can incorporate effect of confinement proposed by [14] shown in Figure 3 is used as the back bone curve. However, for cover concrete unconfined stress-strain relation shown in Figure 3 is used. For concrete in tension a linear uni-axial stress strain relation proposed by [15] is used. For unloading from back bone curve and also for reloading in compression, stress strain relation proposed by [16] shown in Figure 4 is used.

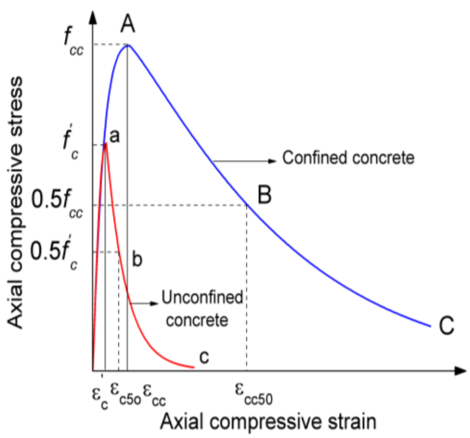

Figure 3: Uni-axial stress-strain relation of confined & unconfined concrete used in analysis

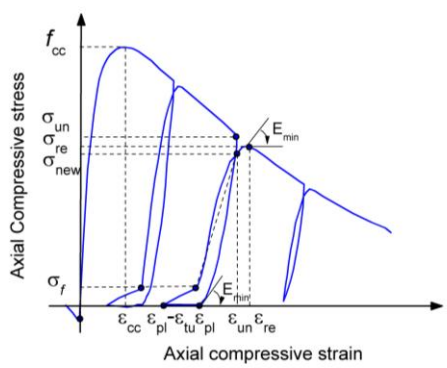

Figure 4: Hysteresis stress-strain relation of concrete used in analysis

For unloading in tension, stress strain relation proposed by [17] is used. This model also used the crack closure function which provides a stiffness recovery procedure from tension to compression and models the crack closure mechanism (Figure 4). Concrete properties and the model parameters used in simulation are given in table 2.

For ordinary and high strength steel a relatively simple relation for monotonic loading proposed by [18] shown in Figures 5(a and b) is used. This model with four parameters is versatile and can simulate different steel behaviors. For hysteretic behavior during cyclic loading a simplified model given by [15] shown in Figure 6 is used. Model parameters of the steels are given in tables (3 and 4).

Table 2: Model parameters used in simulation of concrete

Frame	Concrete
OF/PF	Peak compressive strength = f'_c = 25Mpa, Peak compressive strain = ε'_c = 0.002, Ultimate compressive strength = 0.5 f'_c = 12.5Mpa, Ultimate compressive strain = ε_{c50} = 0.004, Ultimate tensile strength = f_t = 2MPa, Ultimate tensile strain = ε_t = 0.00015, Modulus of elasticity in tension and compression = $E_c = E_t$ = 30GPa

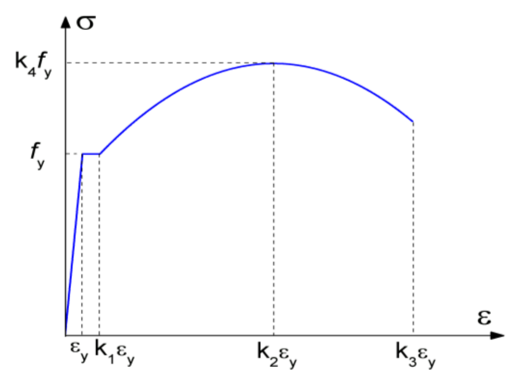

(a)

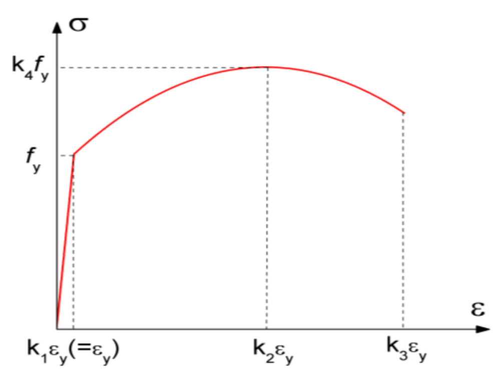

(b)

Figure 5: Monotonic stress strain relation of steel used in analysis

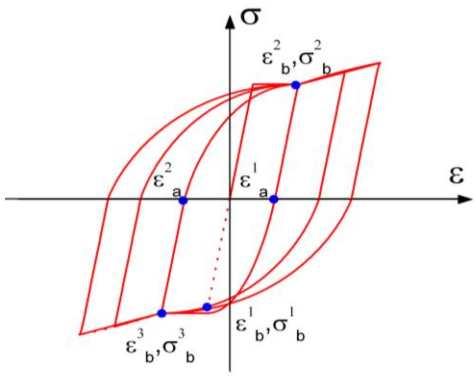

Figure 6: Hysteresis stress-strain relation of steel used in analysis

Table 3: Model parameters used in simulation of ordinary steel

Frame	Ordinary Steel
OF/PF	k_1 = 3.0, k_2 = 25.0, k_3 = 60.0, k_4 = 1.5, Longitudinal steel yield strength = f_y = 400MPa, Stirrup steel yield strength= f_{yh}=350MPa, Modulus of elasticity = E_s = 200GPa Longitudinal steel yield strain=ε_y=0.002

Table 4: Model parameters used in simulation of high strength steel

Frame	High strength steel
PF	k_1 = 2.0, k_2 = 10.0, k_3 = 40.0, k_4 = 1.08, Longitudinal steel yield strength = f_y = 1860MPa, Modulus of elasticity = E_s = 198GPa Longitudinal steel yield strain=ε_y=0.0093

In the analysis the shear strength is assumed large enough and only flexure behavior is considered dominant. Hence the shear deformation and shear failure is neglected. P-delta effects are considered in the analysis.

Beam element is used as finite element in mathematical models. Trial runs are carried out to evaluate the best size of the element in order to avoid localization phenomena as suggested by [15]. Nonlinear static pushover and dynamic time history analysis are used for comparative study.

4. Discussion on pushover analysis

4.1 Damage degree and observed failure mechanism

Frames are analyzed by performing nonlinear static pushover analysis with the inverted triangular lateral loads. Lateral loads are incrementally applied, while the gravity loads are maintained unchanged. For comparative study damage limit states are defined and are related with the observed material strains. Columns are considered critical towards the global stability of the structures. Hence damage degree of the columns and beams is separately marked. High-strength reinforcement has more strength and elastic range than ordinary steel, therefore damage markers in PFs columns are different from OFs. The damage markers for beams are given in table 5 and in table 6 damage markers for the columns are enumerated.

For comparison, pushover curves of the OFs and PFs are drawn in Figure 7. The first instant when severe damage occurred in the OFs is marked and the equivalent damage in the PFs is also shown. The moment when mechanism developed in OFs is marked and the corresponding damage in PFs is also revealed. The instant HSS yields in PFs and the verge of collapse in OFs is also marked. For clarity all the distressed sections at mechanism in OFs and the comparable damage in PFs are shown in Figure 8. To avoid congestion in pictures the markers representing minimal damage are not inserted on beams and columns.

From Figure 7(a) more load and deformation capacity of PF is evident for three story frame. OF has resisted 346kN lateral load at 146mm lateral displacement when severe damage approached (marker 9) the column base. While in PF, 431kN lateral load with substantial damage (marker 4) at the beam end section is observed.

Partial mechanism is observed at 366kN lateral load and 238mm lateral displacement in OF. However, PF resisted 525kN lateral load and only one beam end section at the first floor approached severe damage (marker 5). Yielding initiated at 607kN lateral load and 374mm lateral displacement at the base of first story column in PF. PF lateral load and displacement magnitudes when column base approached yield limit are almost 1.5 times larger than corresponding values at failure mechanism in OF. OF virtually collapsed at 372kN load and at 325mm lateral displacement.

Table 5: Damage markers at beams ends for OF and PF

damage markers	Material strains: Ordinary steel	Material strains: Concrete	Damage	Repair	Structural safety	After repair credible performance
1	$\varepsilon << \varepsilon_y$	$\varepsilon << \varepsilon_o$	Minimal	No Repair		
2	$\varepsilon \leq \varepsilon_y$	$\varepsilon \leq \varepsilon_o$	Light	Repairable	Safe	Satisfactory
3	$\varepsilon_y \leq \varepsilon \leq 0.015$	$\varepsilon \leq \varepsilon_o$	Moderate	Repairable		
4	$0.015 < \varepsilon \leq 0.03$	$\varepsilon_o < \varepsilon \leq \varepsilon_u$	Substantial	Repairable		
5	$0.03 < \varepsilon \leq 0.05$	$\varepsilon \geq \varepsilon_u$	Severe	Excessive		

Table 6: Damage markers at Columns ends for OF and PF

Frame	damage markers	Material strains: Ordinary/High strength steel	Material strains: Concrete	Damage	Repair	Structural safety	After repair credible performance
OF/PF	1	$\varepsilon << \varepsilon_y$	$\varepsilon << \varepsilon_o$	Minimal	No Repair		
OF	6	$\varepsilon_y \leq \varepsilon \leq 0.005$	$\varepsilon \leq \varepsilon_o$	Light	Repairable	Safe	Satisfactory
	7	$0.005 < \varepsilon \leq 0.01$	$\varepsilon_o \leq \varepsilon \leq \varepsilon_u$	Moderate	Repairable		
	8	$0.01 < \varepsilon \leq 0.015$	$\varepsilon_o \leq \varepsilon \leq \varepsilon_u$	Substantial	Excessive	Unsafe	Unsatisfactory
	9	$0.015 < \varepsilon \leq 0.02$	$\varepsilon \geq \varepsilon_u$	Severe	Irreparable		
PF	10	$\varepsilon < \varepsilon_y$	$\varepsilon_o \leq \varepsilon << \varepsilon_u$	Light	Repairable	Safe	Satisfactory
	11	$\varepsilon < \varepsilon_y$	$\varepsilon_o \leq \varepsilon \leq \varepsilon_u$	Moderate	Repairable		

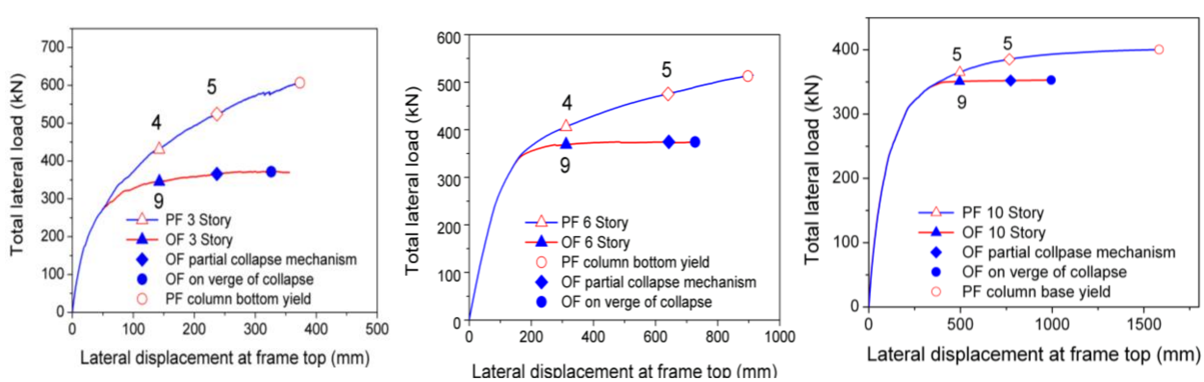

(a) (b) (c)

Figure 7: Nonlinear static pushover analysis curves of OFs and PFs (a) three story frames (b) six story frames (c) ten story frames

Figure 8(a) illustrates that PF columns are saved from yielding and the failure mechanism avoided. In PF first story columns base are moderately damaged (marker 11) as compared with severely damaged columns bases (marker 9) in OF. First and second story columns top in OF suffered light to substantial damage (marker 6 to 8) while minimal damage observed in PF (marker 1).

It is noticeable that the reduced damage in columns of the PF has resulted with increase in the ductility demand at some of the beams ends.

Figure 7(b) indicates more lateral load and deformation capacity of six story PF. Severe damage (marker 9) at the first story columns bases is observed at 347kN lateral load when the frame

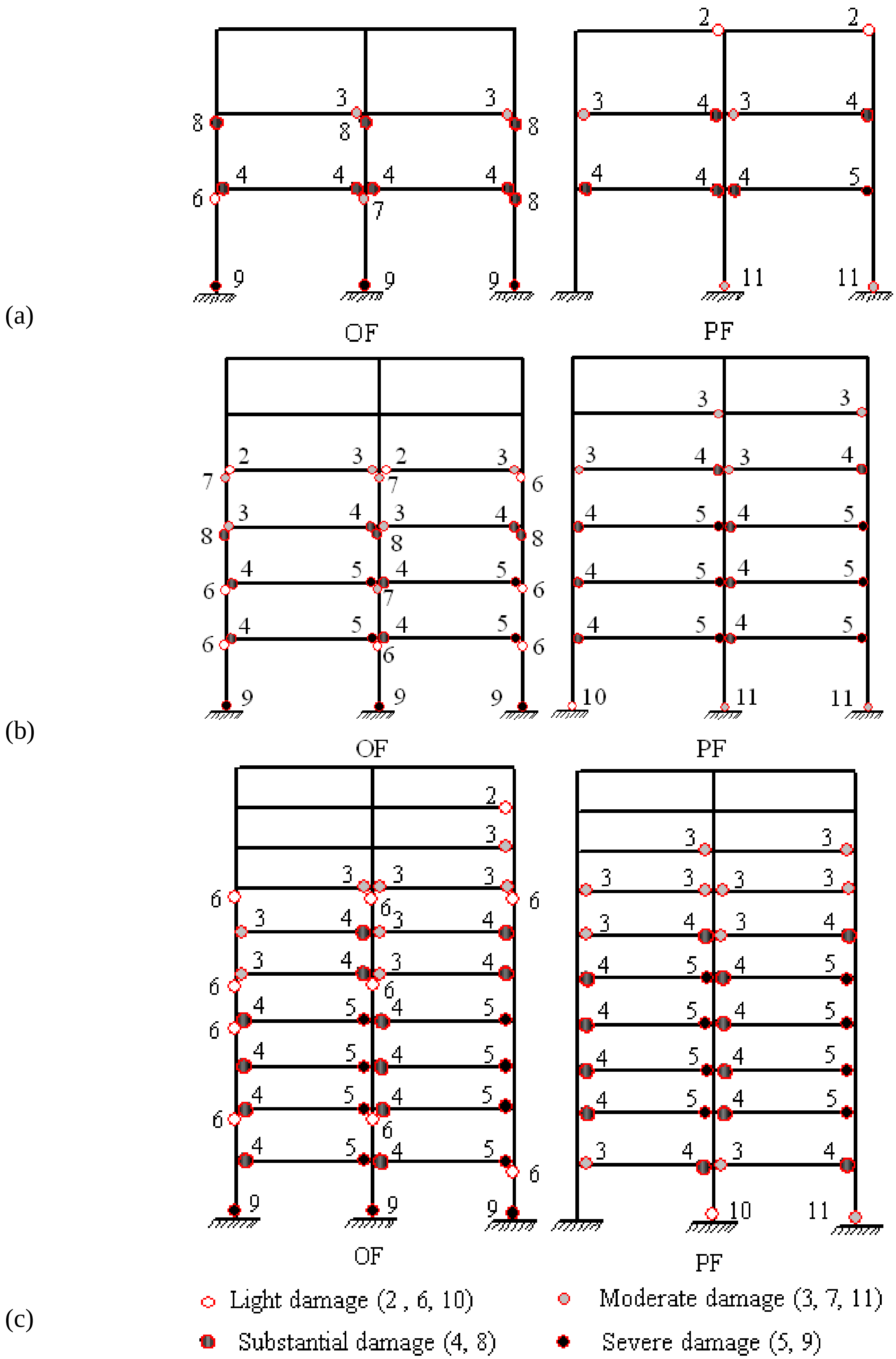

Figure 8: Damage degree of three six and ten story frames

top deformed 226mm laterally. While, PF resisted 383kN lateral load and its beam end section reached substantial damage (marker 4). Mechanism occurred in OF at 356kN lateral load when the top of the frame laterally displaced to 566mm. At this stage PF resisted 480kN lateral load and mechanism remained absent. However the beams end sections reached severe damage (marker 5). PF column bottoms approached yielding at 506kN lateral load and at 751mm lateral displacement which is almost 1.4 times larger in magnitudes than the corresponding values observed at mechanism in OF.

Damage markers in Figure 8(b) highlight the reduced damage degree of PF. The columns are saved from yielding in PF, while severe yielding occurred in columns of the OF. Partial mechanism observed in OF because of the severe yielding at the columns bases (marker 9) and at the top of fourth story columns (marker 8). However columns bases in PF showed moderate damage (marker 11). It is also noticeable that beam ends in both the frames showed comparable damage.

For the ten story frames large deformation capacity of PF is again evident (Figure 7(c)). At 351kN lateral load and 495mm lateral displacement OF column bottom reached severe damage (marker 9). However PF beam end section showed severe damage (marker 5) and the lateral load magnitude observed is 367kN. Further load increment increased damage at the columns bases without much increase in the load resistance in OF and mechanism is observed at 352kN load and at 774mm lateral displacement. While PF, still showed damage concentration at the beams ends (marker 5) and has resisted 385kN lateral load. PF reached the yielding at the columns bases at 400kN lateral load and at 1584mm lateral displacement. OF completely collapsed because of columns base failures at 353kN lateral load and 995mm lateral displacement. It is noticeable that the lateral deformation capacity of PF at the initiation of yielding is almost 2.0 times larger than OF at the start of mechanism and the loading resistance is almost 1.13 times larger than OF.

Figure 8(c) illustrates comparable damage at the beam ends between OF and PF. However severe damage at the columns bases of the first story columns (marker 9) and yielding at the top of the sixth and seventh story columns (marker 6) is observed in OF. Partial mechanism declared in OF at the moment when maximum useable strain limits of 0.02 in compression and 0.05 in tension (FEMA-356) [20] crossed. Since the load increment resulted with large strains at the columns bases without further increase in load resistance. In contrast PF columns showed light damage (marker 10). Absence of yielding in the columns not only provided lateral load resistance but also delayed formation of failure mechanism in PF.

5. Time History Analysis

For studying dynamic response, Northridge earthquake is used as dynamic input. Time acceleration record shown in Figure 9 is downloaded from Pacific Earthquake Engineering Research Centre (PEER 2000) strong motion database. Time history analysis with the time step length of 0.01sec is used. Rayleigh's damping with the damping coefficient 5% of the critical is used. First two modes of vibration are used for calculating mass and stiffness matrix multipliers. Fundamental periods of vibration for the three, six and ten story frames are 0.48, 0.91 and 1.48 seconds respectively. Degree of damage, top displacement history, residual displacements, maximum interstory drift and maximum floor accelerations are compared for OFs and PFs.

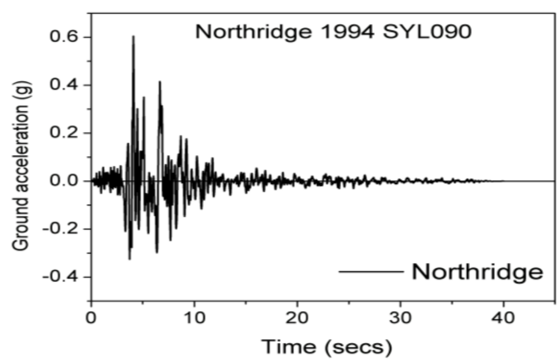

Figure 9: Time acceleration records of Northridge earthquake

6. Discussion on Dynamic Response

6.1 Damage degree and observed failure mechanism

Damage degree is marked and is shown in Figure 10. Three story OF suffered substantial to severe damage (marker 8 to 9) at the first story columns bases and light to moderate damage at the top of the first and second story columns (marker 6 to 7). In contrast, PF showed absence of yielding in all the columns (Figure 10(a)). First story columns bases in PF suffered light damage (marker 10).

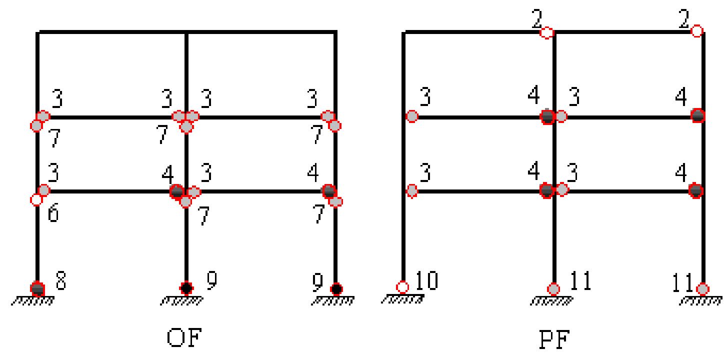

(a)

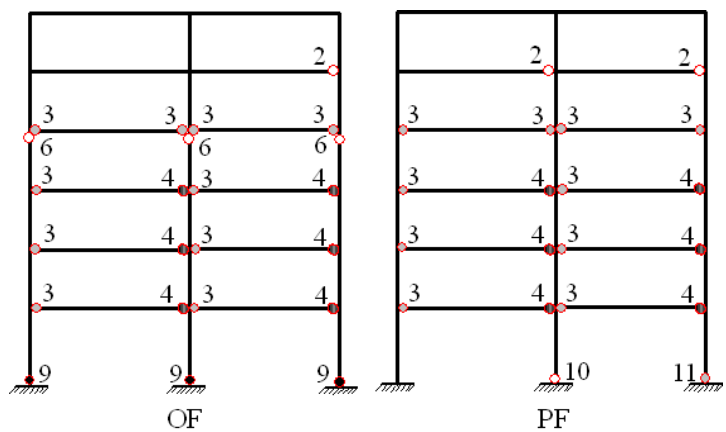

(b)

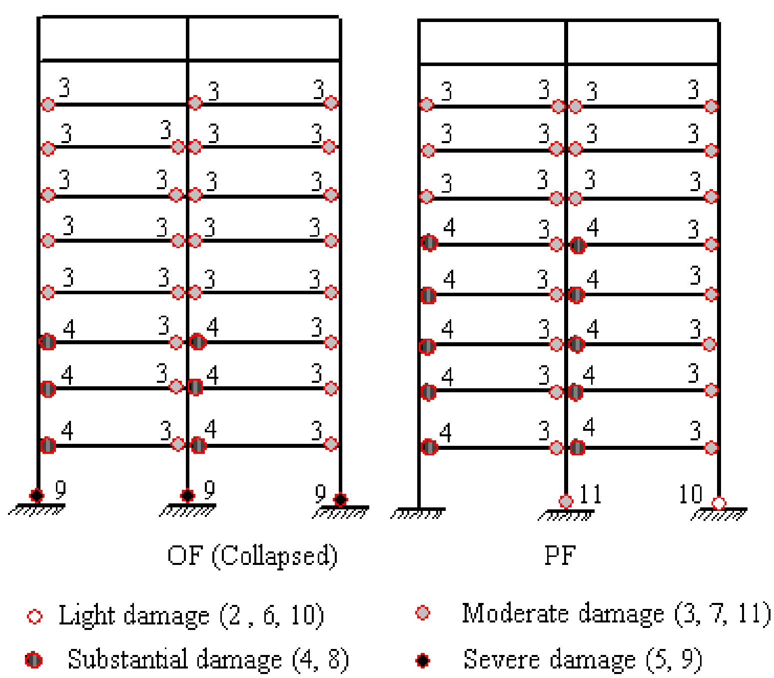

(c)

Figure10: Damage degree of three, six and ten story frames (Northridge earthquake response)

Some of the beams ends in PF showed more distress as compared with OF. More yielding at the beams ends in PF demonstrates the increase in the ductility demands. This demand can be fulfilled by providing confinement at the beam ends.

Figure 10(b) illustrates the damage in the six story frames. In OF severe damage (marker 9) is apparent at the first story columns bases. Further at the top of fourth story columns light damage (marker 6) is observed. This formation of plastic hinges highlights imminence of the partial mechanism. While in PF because of more flexural strength of columns, damage is seen confined at the beam ends only and all the columns are saved from yielding. Damage degree of ten story frames is shown in Figure 10(c). Since OF virtually collapsed and results did not converge. Damage occurred in OF till 6.6secs of simulation is compared with PF. Since afterwards all the critical sections showed severe damage. Bottom of the first story columns in OF showed severe damage (maker 9) while the columns in the above stories showed minimal damage. PF showed light to moderate damage (marker 10 to 11) in the first story columns at base. Beams in the lower stories in PF showed slightly more damage than OF. Although the difference in damage degree in beams between OF and PF is not as significant but excessive damage at the columns bases in OF formed total failure mechanism. While in PF, large deformation capacity of columns delayed formation of total mechanism.

6.2 Top Displacement History

The top displacement histories are shown in Figures 11. For the three story frames (Figure 11(a)), the difference is less obvious at the top. Since excessive yielding at the columns bases and at the top of second story columns resulted in partial mechanism in OF. Hence, the top story of the OF moved like a rigid body without much of the relative lateral deformations. However, in contrast inelastic deformations did not concentrate at one particular floor in PF. It can also be stated that absence of yielding in the columns of PF does not increase the maximum lateral displacement response.

From Figures 11(b) less lateral shift from origin is evident in PF. Smaller lateral shift during oscillations is the result of virtually elastic columns of the PF. A good agreement between maximum lateral displacements is also noticed.

Ten story frames top displacement history is shown in Figure 11(c). OF virtually collapsed and results did not converge after 9sec. More deformation capacity of the columns of PF prevented permanent drift from the zero position.

6.3 Residual lateral displacement

Frames are analyzed for period more than dynamic input. Residual displacements shown in Figures 12 are observed when the oscillations almost ceased in frames. For the three story frames the reduced residual lateral displacements are attained in PF (Figure 12(a)). Residual displacements for the six story frames also stress the lowering in residual displacements in PF (Figure 12(b)). For the ten story frames residual displacements of the PF are shown in Figure 12(c). Since OF approached dynamic instability and results did not converge. It is also interesting to note that at the first story the residual displacements are negligible in PFs.

6.4 Interstory Drift Response

In this study maximum interstory drift response is also compared for rational comparison. The observed maximum interstory drifts are drawn in Figures 13.

Three story OF showed considerably more drift magnitudes at the first story as compared with PF (Figure 13(a)). In the second and third stories maximum interstory drift magnitude is observed more in PF. Since partial mechanism approached in OF and third story columns showed less relative displacements. Comparison of maximum interstory drift magnitude in the frames revealed more response in OF. Six story frames indicates more drift at the first and second story in OF (Figure 13(b)). However, relatively more magnitude is observed in the above stories of the PF. Because of the absence of yielding in PF columns slight increase in drift in the above stories is understandable. Maximum interstory drifts for ten story OF shown in Figure 13(c) are at 6.6sec of the simulation time, before approaching collapse mechanism. It is evident from results that first story failure mechanism approached in OF. PF, however showed steady response and maximum interstory drift occurred at the third story.

6.5 Maximum floor acceleration response

A large portion of non structural components and building contents are damaged primarily as a result

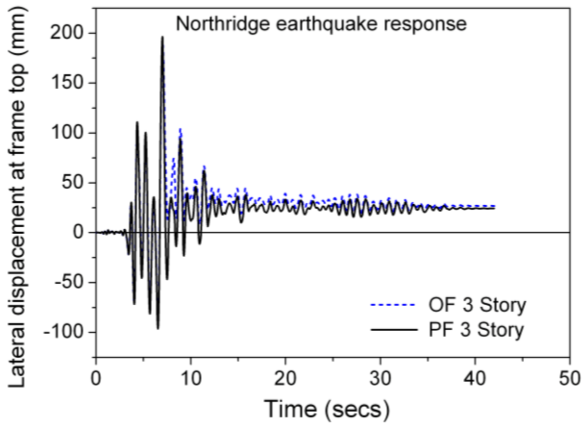

(a)

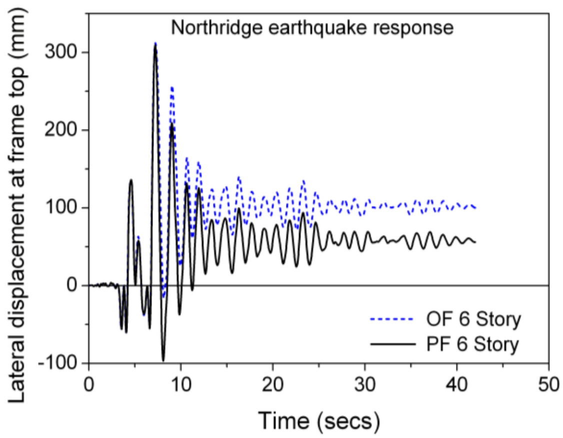

(b)

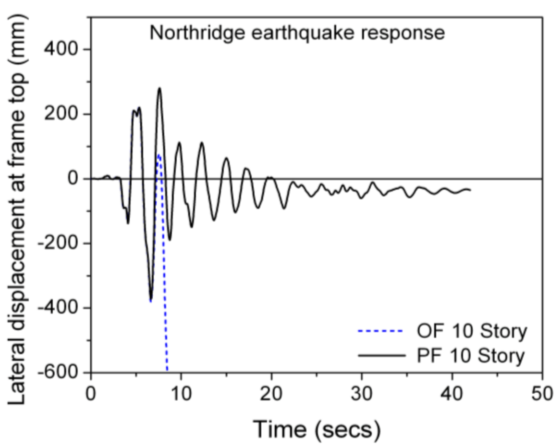

(c)

Figure 11: Time lateral displacement response (a) three story (b) six story (c) ten story Northridge earthquake response of OFs and PFs

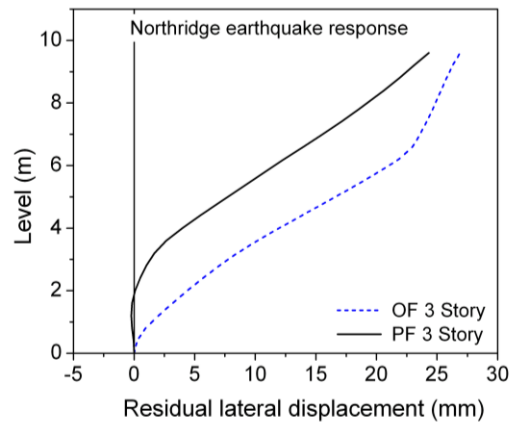

(a)

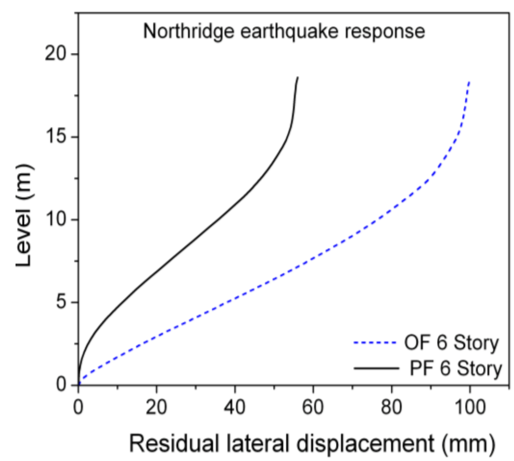

(b)

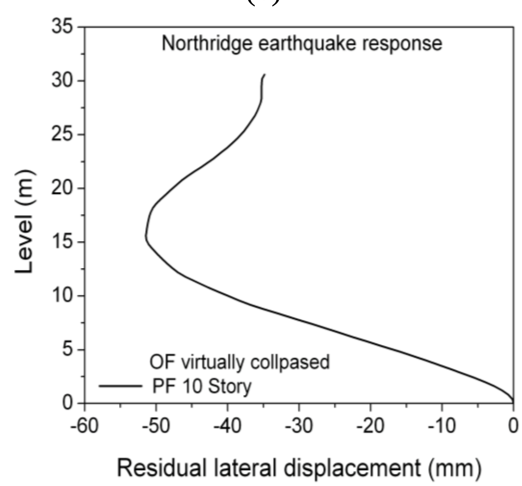

(c)

Figure 12: Residual lateral displacements at the end of the dynamic response of OFs and PFs (a) three story frames (b) six story frames (c) ten story frames Northridge earthquake response

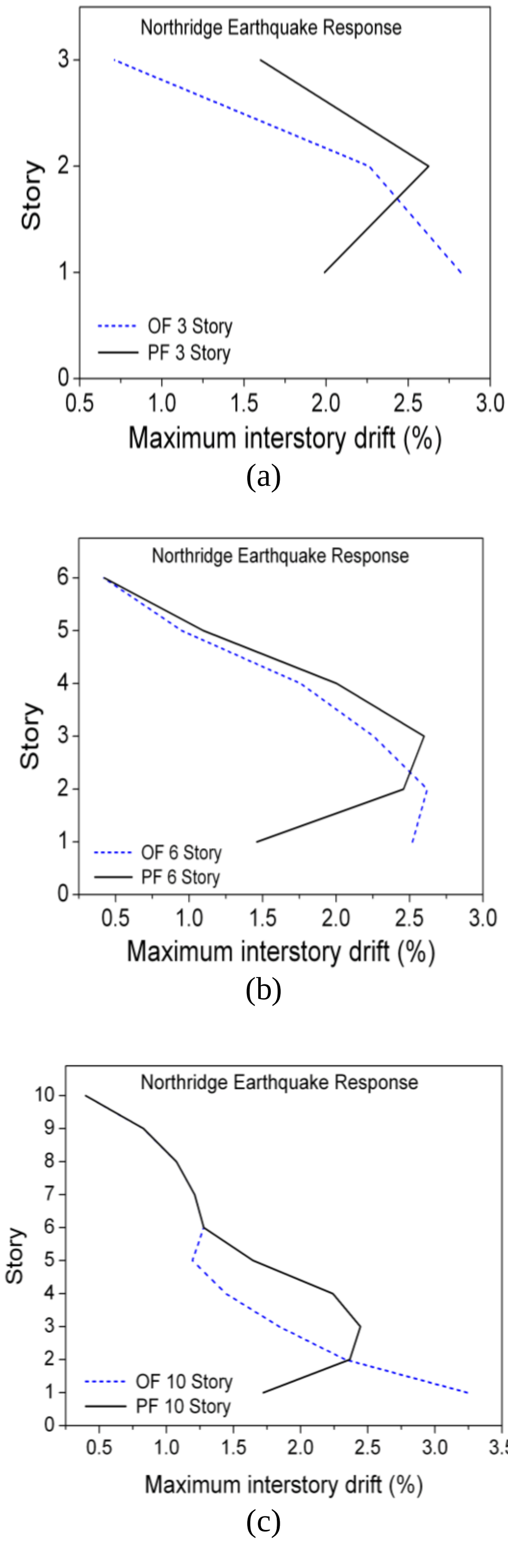

Figure 13: Maximum interstory drift response of OFs and PFs (a) three story frames (b) six story frames (c) ten story frames Northridge earthquake response

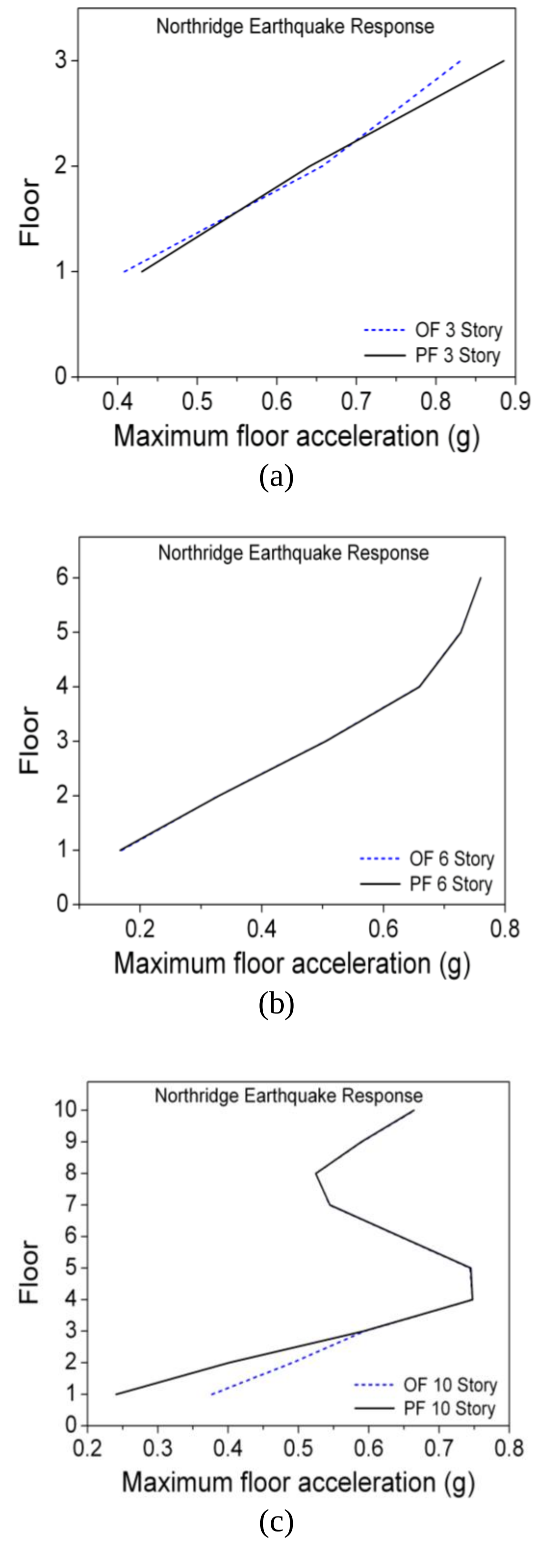

Figure 14: Maximum floor acceleration response of OFs & PFs (a) three story frames (b) six story frames (c) ten story frames Northridge earthquake response

of being subjected to large floor acceleration demands [21]. Maximum floor acceleration response is compared and is shown in Figure 14.

It is evident from Figure 14(a) that the three story frames responded with a little difference. Six story frames also showed exact similarity in response between OF and PF (Figure 14(b)). Maximum floor acceleration response of ten story frame also revealed almost similarity in response in the above floors between OF and PF. However, in the first and second floor relatively more response is observed in OF before approaching collapse mechanism (Figure 14(c)).

Hence from the above observations in general, a similarity in the acceleration response between OF and PF can be inferred.

7. Conclusions

To determine the response benefits of HSS reinforcements in frame construction, non linear static pushover and time history analysis are performed. For detailed investigation two bays three, six and ten story frames are selected. Based on the analysis results following conclusions can be drawn.

1. In the small to medium rise frames HSS reinforcements in the frame columns can provide more lateral strength and deformation capacity against lateral loadings. However, for high rise frames increase in deformation capacity is more obvious than the strength increase by the use of HSS reinforcements in the columns.

2. Damage degree in the ordinary steel reinforced concrete construction can be reduced by replacing the ordinary reinforcement with HSS. Soft story and partial failure mechanism can be prevented and total or sway failure mechanism can be delayed by utilizing HSS reinforcements in columns.

3. Residual displacements at the end of dynamic event can be minimized by using HSS reinforcements.

4. The absence of yielding in columns because of HSS may also increase ductility demands at the beams ends.

5. Frame response is observed by simple replacement of ordinary reinforcement with HSS. However, in the future study various parameters such as beam column stiffness ratios, beam column strength ratios and shear strength demands because of HSS reinforcement needs to be investigated.

8. References

[1] Dinh, T. V. and Ichinose T; *Journal of Structural Engineering*, 131-3(2005) 416-427.

[2] Paulay, T. and Priestley M. J. N; *Seismic design of reinforced concrete and masonry buildings*, Wiley, New York, (1992).

[3] Fischer, G., and Li, V. C; *ACI Structural journal*, 100-2 (2003) 166-176.

[4] Priestley, M. J. N., Sritharan, S. S., Conley, J. R. and Pampanin S; Precast/Prestressed Concrete Institute Journal, 44-6 (1999) 42-67.

[5] El-Sheikh, M.T., Sause, R., Pessiki, S. and Lu, L. W; Precast/Prestressed Concrete Institute Journal, 44 -3(1999) 54-71.

[6] Kurama, Y. C., Pessiki, S., Sause, R. and Lu L. W; Precast/Prestressed Concrete Institute Journal, 44-3(1999) 72-89.

[7] Ricles, J. M., Sause, R., Garlock, M. M. and Zhao, C; Journal of Structural Engineering, 127-2(2001) 113-121.

[8] Kwan, W. P. and Billington, S. L; Journal of Bridge Engineering, 8-2 (2003) 92-101.

[9] Lu Y; *Journal of Structural Engineering*, 128-2(2002) 169-178.

[10] Dooley, L. and Bracci, J. M; *ACI Structural Journal*, 98-6(2001) 834-851.

[11] American Concrete Institute (ACI); Building code requirements for structural concrete and commentary, Detroit, (2002) *ACI 318-02*.

[12] Lu, X. Z., Miao, Z. W., Huang, Y. L. and Ye, L. P; *Proc., MSC. Software Chinese Users' Conference*, Chengdu, China, (2005), 1-10.

[13] Wang, X. L., Lu, X. Z., Ye, L. P; *Earthquake Resistant Engineering and Retrofitting*, 28-6(2006) 25-29.

[14] Legeron, F. and Paultre, P; *Journal of Structural Engineering*, 129-2(2003) 241-252.

[15] Legeron, F., Paultre, P., Mazars, J; *Journal of Structural Engineering*, 131-6(2005) 946-955.

[16] Mander, J. B., Priestley, M. J. N. and Park, R. *Journal of Structural Engineering*, 114-8(1988) 1804–1825.

[17] Miranda, E. and Taghavi, S; *Journal of Structural Engineering*, 131-2(2005) 203-211.

[18] Esmaeily, A. and Xiao, Y; *ACI Structural Journal*, 102-5(2005) 736–744.

[19] http://peer.berkeley.edu/smcat/search.html assessed 10 June 2007.

[20] Federal Emergency Management Agency (FEMA); Prestandard and commentary for the seismic rehabilitation of buildings, Washington, D. C, (2000), *FEMA-356.*

[21] Miranda, E. and Taghavi, S; *Journal of Structural Engineering*, 131-2(2005) 203-211.